

RSC Advances



This is an *Accepted Manuscript*, which has been through the Royal Society of Chemistry peer review process and has been accepted for publication.

Accepted Manuscripts are published online shortly after acceptance, before technical editing, formatting and proof reading. Using this free service, authors can make their results available to the community, in citable form, before we publish the edited article. This *Accepted Manuscript* will be replaced by the edited, formatted and paginated article as soon as this is available.

You can find more information about *Accepted Manuscripts* in the [Information for Authors](#).

Please note that technical editing may introduce minor changes to the text and/or graphics, which may alter content. The journal's standard [Terms & Conditions](#) and the [Ethical guidelines](#) still apply. In no event shall the Royal Society of Chemistry be held responsible for any errors or omissions in this *Accepted Manuscript* or any consequences arising from the use of any information it contains.

Capillary isotachophoresis for separation of silver nanoparticles according to size

Petr Praus^{a,b*}, Martina Turicová^a, Petr Suchomel^c, Libor Kvítek^c

^aDepartment of Chemistry, VŠB-Technical University of Ostrava, 17. listopadu 15, 708 33 Ostrava-Poruba, Czech Republic

^bInstitute of Environmental Technology, VŠB-Technical University of Ostrava, 17. listopadu 15, 708 33 Ostrava-Poruba, Czech Republic

^cDepartment of Physical Chemistry, Palacký University, 17. listopadu 12, 771 46 Olomouc, Czech Republic

Abstract

Capillary isotachophoresis (ITP) was used for the separation of Ag nanoparticles according to their size. For this purpose the ethanol-water dispersions of Ag nanoparticles stabilized by gelatin were prepared. The ITP separations were performed in a column-coupling system filled with two electrolytes with pH of leading electrolytes of 7.1 (system I – LE: 10 mM HNO₃, ε-aminocaproic acid, TE: 10 mM caproic acid) and 4.5 (system II – LE: 10 mM HNO₃, imidazole, TE: 5 mM 2-(*N*-morpholino)ethanesulfonic acid). In the both electrolyte systems the four main peak-mode zones of Ag nanoparticles migrating at zone boundaries were identified, however, the better separation was achieved in the system II. The Ag nanoparticles dispersions were also examined by dynamic light scattering (DLS) and transmission electron microscopy (TEM). Zeta potential and thickness of gelatin double layers adsorbed on the nanoparticles were found to depend on pH. The TEM analysis revealed the four size fractions of 4 nm, 10 nm, 16 nm and 22 nm, which correspond to the zones separated by ITP. Other migration zones of the electrolyte systems, such as impurities and/or products of the nanoparticle synthesis, served as spacers separated the peak zones of Ag nanoparticles.

Key words: Capillary isotachophoresis, silver nanoparticles, gelatin, separation, size

* Corresponding author. Tel: +420-59-732-1675. E-mail address: petr.praus@vsb.cz

Introduction

Over more than 30 years nanomaterials have been intensively studied due to their excellent properties utilized in many science and industrial fields, such as optics, electronics, magnetic applications, solar energy conversion, medicine, environmental protection, chemistry including catalysis etc. For all these applications nanoparticles size distribution is the basic characteristic. It can be determined by several common methods, such as transmission and scanning electron microscopy, atomic force microscopy, dynamic light scattering, laser diffraction, photon correlation spectroscopy, field flow fractionation¹ and asymmetrical flow field flow fractionation,² centrifuged particles size analysis³, hydrodynamic chromatography, size exclusion chromatography⁴ and also by gel and capillary zone electrophoresis (CZE).⁵

Utilization of CZE for the study of nanoparticles size distribution has been recently reviewed in several papers.⁶⁻¹⁴ Quantum dots, noble metals (gold and silver) nanoparticles, carbon nanotubes, metal-oxide particles (Al_2O_3 , TiO_2 , Fe_2O_3), latex and polystyrene particles, silica nanoparticles and nanoparticle-biomolecule conjugates were the most often separated nanoparticles.

Capillary isotachopheresis is well developed electrophoretic technique in which a sample is injected between leading and termination electrolyte. Ions are separated in zones with sharp boundaries moving with the same velocity. The concentrations of separated ions in their zones are adapted to the concentration of the leading ion. The loading capacity of ITP is several times higher than capacity of CZE, therefore, both methods are also used to be connected (ITP-CZE) with very high separation efficiency. ITP and/or ITP-CZE were applied for separation of quantum dots^{6,15-19} and gold nanoparticles.¹⁶ ITP was also tested for the separation of micelles of cetyltrimethylammonium bromide²⁰ and micron sized particles.²¹

By our best knowledge silver nanoparticles have not been separated by ITP yet. Therefore, the aim of this paper was to use ITP for determination of the size distribution of silver nanoparticles stabilized by gelatin in ethanol-water colloid dispersions. The ITP experiments were completed with TEM and DLS analyses. Electrophoretic mobilities of separated fractions were calculated from the ITP records and discussed in context of the theory of electrophoretic mobility of colloidal particles.

Experimental

Chemicals

All chemicals were of analytical reagent grade: nitric acid, caproic acid, ϵ -aminocaproic acid (EACA) (all from Lachema, Czech Republic), β -alanine, 2-(*N*-morpholino)ethanesulfonic acid (MES) (Serva, Germany), imidazole (Sigma-Aldrich), silver nitrate (Sigma-Aldrich), gelatin (Fluka), ethanol (LachNer), ammonia (Sigma-Aldrich), sodium hydroxide (Penta) and maltose (Sigma-Aldrich). Twice distilled and deionised water by a mixed-bed ion-exchanger was used for preparation of all ITP electrolytes. The compositions of leading (LE) and terminating (TE) electrolytes are given in Table I.

Table I ITP Electrolyte systems

Parameter	Electrolyte systems	
	I	II
Leading anion	NO ₃ ⁻	NO ₃ ⁻
Concentration (mmol l ⁻¹)	10	10
Counter ion	Imidazole	EACA
pH (LE)	7.10	4.50
Terminating anion	MES	Caproic acid
Concentration (mmol l ⁻¹)	10	5
pH (TE)	4.30	3.80

Preparation of silver nanoparticles

Silver nanoparticles in ethanol-water solvent (ethanol mixed with demineralised water 2:3) were prepared by the modified Tollens process²² and stabilized by natural polymer gelatin to prevent their aggregation. 5 ml of 5·mmol l⁻¹ AgNO₃ was diluted with 2.75 ml of gelatin solution (72.7 g l⁻¹), placed on a magnetic stirrer and vigorously stirred. Then, 10 ml of ethanol was added into the solution. Still under vigorous stirring, 1.25 ml of 0.1 mol l⁻¹ ammonia was rapidly injected and a solution mixed by 5 ml of 0.05 mol l⁻¹ maltose with 1 ml of 0.24 mol l⁻¹ sodium hydroxide was added. After adding of the reaction components, the solution was stirred for a further 30 minutes, than the prepared dispersion of silver nanoparticles was placed into plastic tubes and left aged for 24 hours.

Isotachophoretic separation

An isotachophoretic analyzer EA 102 (Villa-Labeco, Slovakia) in the column-coupling configuration was employed. The capillaries were made from a fluorinated ethylene-propylene copolymer (FEP): a pre-separation capillary 90 x 0.8 mm I.D and an analytical capillary 200 x 0.3 mm I.D. Both capillaries were equipped with contact conductivity detectors and, in addition, the analytical capillary was equipped with an UV detector. The driving current in the pre-separation capillary was set at 250 μ A and in the analytical capillary at 50 μ A in all experiments. Samples were injected through a 30 μ l sampling loop. The pH values of the electrolyte systems were measured with a pH metre WTW InoLab (Weilheim, Germany).

Absorption molecular UV-VIS spectrometry

UV-VIS absorption spectra were measured by a double-beam spectrometer Lambda 25 (Perkin Elmer, USA). All spectra were recorded using 1 cm quartz cuvettes within the range of 200 nm to 800 nm. The cuvettes were filled with the 10 times diluted Ag aqueous dispersions with water and their absorption spectra were recorded.

Electron transmission microscopy

Transmission electron microscopy of Ag nanoparticles was performed by a JEM 220FS microscope (Jeol, Japan) operating at 200 kV. The Ag nanoparticles were dispersed in ethanol and with ultrasonic sprayer deposited on a TEM grid with carbon holey support film.

Zeta-potential measurement

Zeta-potential of silver nanoparticles was determined using Zetasizer Nano ZS (Malvern Instruments Ltd, England) instrument in disposable capillary cell via Electrophoretic Light Scattering method. The zeta-potential of silver nanoparticles was measured in the primarily prepared dispersions after dilution 1:9 using demineralised water and the leading electrolytes to modify their pH values.

Results and discussion

In general, electrophoretic mobility m of colloidal particles is not easy to express. Colloidal particles can be considered as spherical particles with radii r surrounded by electric double layers of the thickness $1/\kappa$, where the parameter κ is proportional to the square root of ionic strength of bulk solution. Depending on dimensionless quantity κr , two limiting cases were

theoretically derived. First, when κr is very small ($\kappa r < 1$) the charged particles can be considered as point charges, Hückel derived the electrophoretic mobility as follows²³

$$m = \frac{\varepsilon_r \varepsilon_0 \zeta}{1.5\eta} \quad (2)$$

where ε_r and ε_0 are the relative and vacuum permittivity, respectively, ζ is the zeta potential, η is the dynamic viscosity of dispersion medium. Second, when κr is large ($\kappa r \gg 1$), the double layer is supposed to be flat and Smoluchowsky derived the electrophoretic mobility as

$$m = \frac{\varepsilon_r \varepsilon_0 \zeta}{\eta} \quad (3)$$

In these limit conditions the electrophoretic mobility does not depend on the particle radius. For, let us say, real conditions, Henry derived the equation taking into account the particle radius as well as the double layer thickness as

$$m = \frac{\varepsilon_r \varepsilon_0 \zeta}{1.5\eta} [1 + \lambda F(r\kappa)] \quad (4)$$

where λ depends on conductivity of bulk solution and the function $F(r\kappa)$ varies from 0 to 1. For nonconducting particles the Henry equation (4) can be simplified as

$$m = \frac{\varepsilon_r \varepsilon_0 \zeta}{1.5\eta} f(r\kappa) \quad (5)$$

where $f(r\kappa)$ is a dimensionless function varying from 1 to 1.5 and also depending on shape of particles. For the product $r\kappa$ in the interval from 0.1 to 10^3 the function $f(r\kappa)$ is increasing for spherical particles. For cylindrical particles the function $f(r\kappa)$ can increase or decrease depending on their orientation towards electric field.^{23,24}

These classical models were completed by Wiersema et al.²⁵ who showed that in the range of $1 < r\kappa < 10$ for zeta potentials higher than 78 mV the electrophoretic mobility of colloid particles has a minimum. This model explains reciprocal relationships between the electrophoretic mobility and the particles sizes reported in several papers.^{17,26-28}

Isotachophoretic separation

Isotachophoretic separations of Ag nanoparticles dispersions containing 40 % (v/v) of ethanol and stabilized by gelatin were performed by the two columns coupled system using two electrolyte systems with the different pH values (Tab. I) and with no additives for suppression of electroosmotic flow. Gelatin was used for the stabilization due to its long term stability in a broad range of pH.²⁹

The isotachophoretic separations recorded by conductivity and UV-VIS detectors are shown in Figures 1a and 1b. One ITP run the two-columns system took about 25 minutes. These figures also show ITP records of blank separations, in which the terminating electrolyte was injected instead of Ag dispersions. The time difference between the conductivity and UV-VIS detector was about 39 seconds. Therefore, the ITP records in Figures 1 were shifted to correct this difference and to simplify the zone identification. The zones were also identified by the separation of Ag dispersions of different dilutions. In order to verify the ITP steady state was reached the calibration plots of absorption peak area against the reciprocal value of dilution of the origin Ag colloid were constructed (Fig. 2). It was performed for the separation in the system II when the resolution of Ag nanoparticles peaks was better than in the system I. Their good linearity proves the correct ITP separation.

Table II Electrophoretic mobilities of Ag nanoparticles in systems I a II

Zone No./syst. I	$m_{Ag} \times 10^{-9} \text{ (m}^2\text{V}^{-1} \text{ s}^{-1}\text{)}$	Average $\times 10^{-9} \text{ (m}^2\text{V}^{-1} \text{ s}^{-1}\text{)}$
1	-66.0 to -55.5	-60.8
2	-54.0 to -49.3	-51.7
3	-49.3 to -45.6	-47.5
4	-45.6 to -41.7	-43.7
Zone No./syst. II	$m_{Ag} \times 10^{-9} \text{ (m}^2\text{V}^{-1} \text{ s}^{-1}\text{)}$	Average $\times 10^{-9} \text{ (m}^2\text{V}^{-1} \text{ s}^{-1}\text{)}$
1	-61.3 to -47.5	-54.4
2	-47.5 to -42.6	-45.1
3	-42.6 to -35.5	-39.1
4	-31.9 to -25.7	-28.8

In both electrolyte systems, four main peak-mode zones³⁰ of Ag nanoparticles were observed at the boundaries between other ITP zones of electrolyte impurities (denoted as x and xx), ions left from the nanoparticles synthesis and free gelatin. The similar peak-mode

zones have been observed in case of gold nanoparticles¹⁶ as well as micron sized particles.²¹ In general, the separation of nanoparticles in their pure ITP zones is not possible due to approximately Gaussian distributions of their sizes which is visible in the UV-VIS detector records.

In order to determine the electrophoretic mobilities of Ag nanoparticles m_{Ag} their upper and lower mobility limits were estimated from conductivity signals of neighbouring zones as follows

$$m_i = \frac{m_{LE} \kappa_i}{\kappa_{LE}} \quad (6)$$

where m_{LE} is the electrophoretic mobility of leading anion which was nitrate ($-74.1 \cdot 10^{-9} \text{ m}^2\text{V}^{-1} \text{ s}^{-1}$), κ_i and κ_{LE} are the conductivity signals of a zone i and leading zones, respectively. The results are summarized in Table II. The average mobilities from the lower and upper ones were calculated as well. The silver nanoparticles mobilities were determined with uncertainty of RSD = 5.9 % (n = 27) and RSD = 11.9 % (n = 16) in the system I and II, respectively.

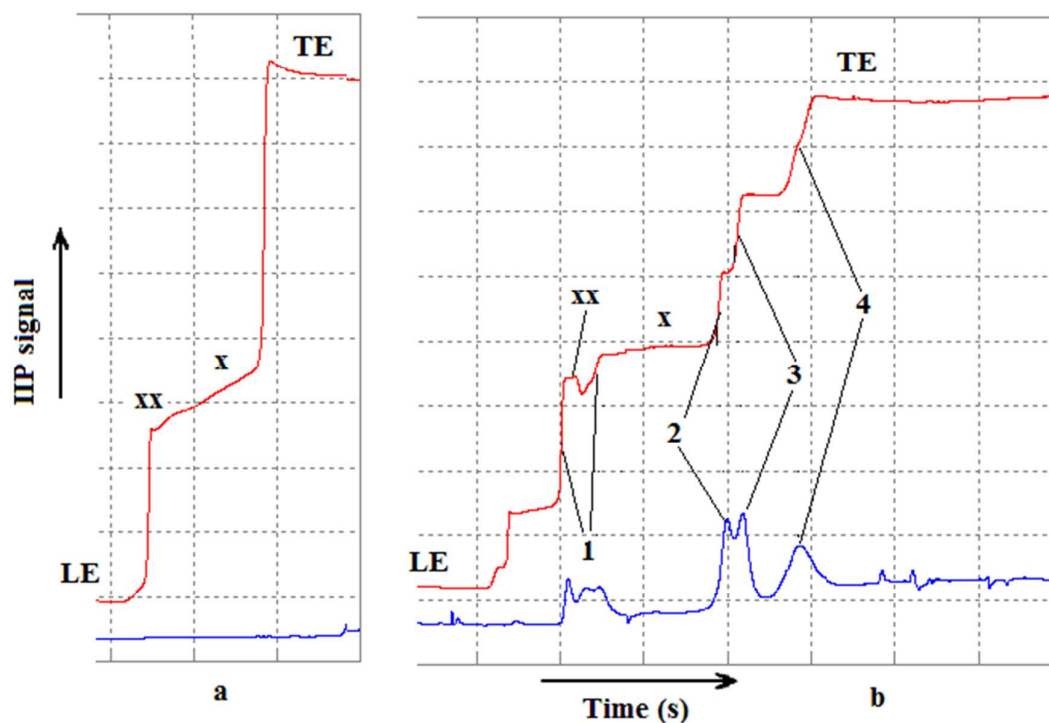


Figure 1a ITP separation records in electrolyte systems I. a – blank, b – Ag nanoparticles. The zones x and xx are impurities of the electrolyte system.

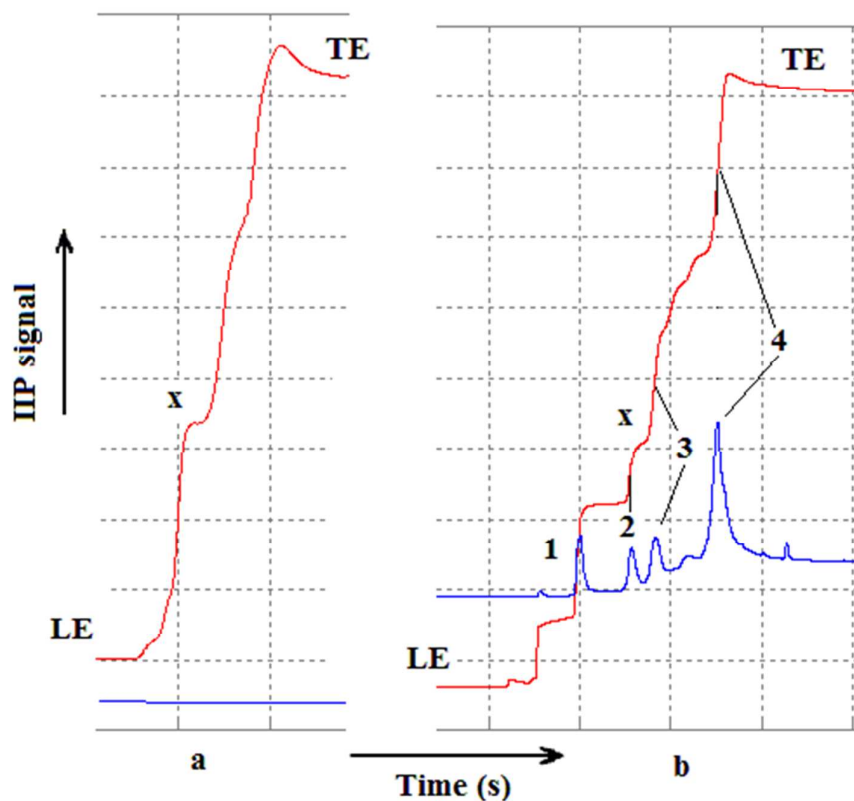


Figure 1b ITP separation records of Ag nanoparticles in electrolyte systems II. a – blank, b – Ag nanoparticles. The zone x is an impurity of the electrolyte system.

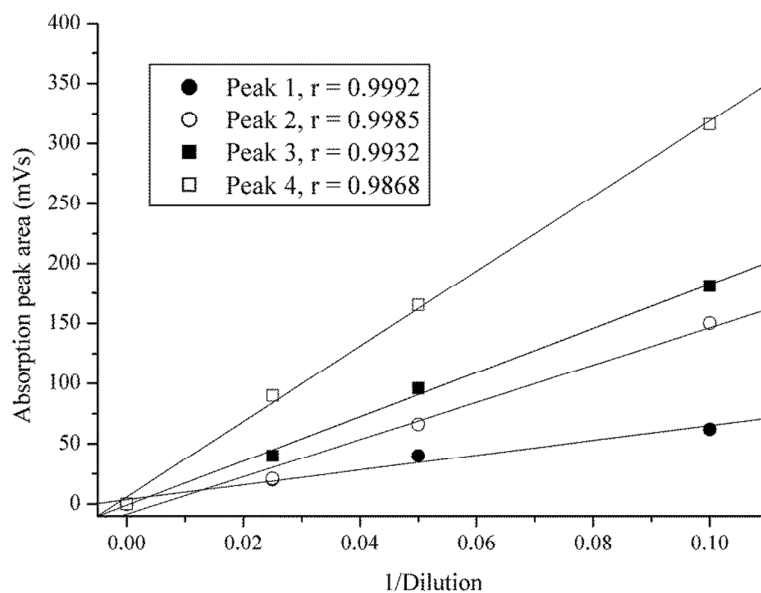


Figure 2 Dependence of absorption peak area on reciprocal value of dilution of the original Ag colloid separated in the system II (r – regression coefficient)

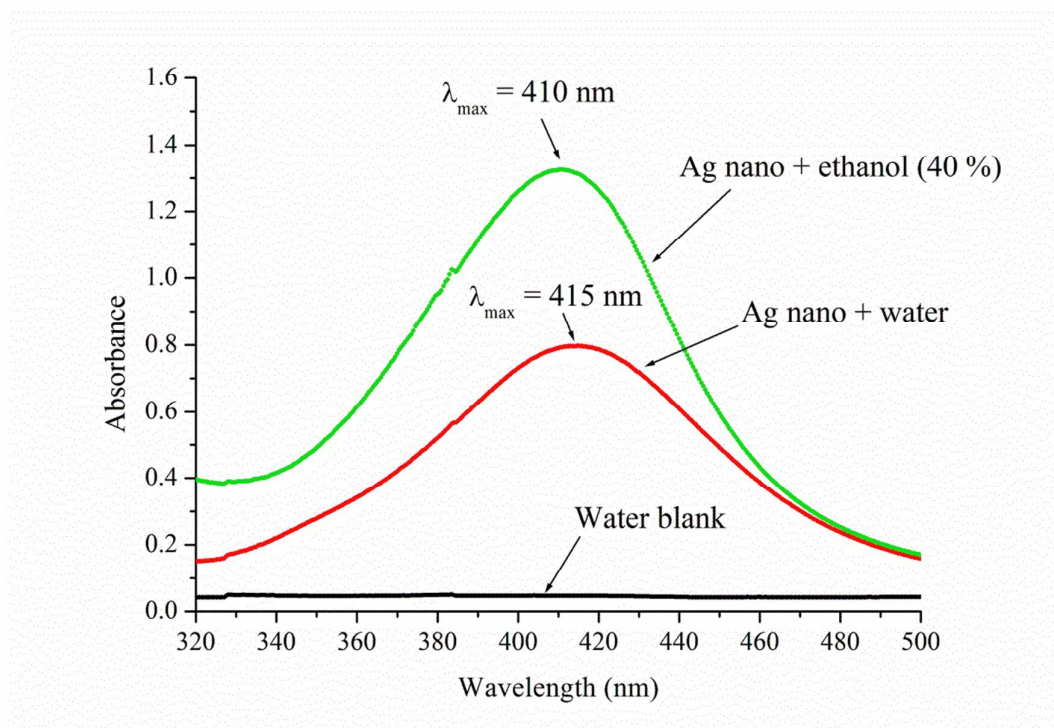


Figure 3 UV-VIS spectra of Ag colloids stabilized by gelatin in water and ethanol

The detection wavelength of 410 nm corresponded to the absorption maxima of the Ag dispersion stabilized by gelatin in the ethanol-water solutions (40 % ethanol) shown in Figure 3. Due to dilution of the Ag dispersions during the ITP separation the absorption spectrum of Ag nanoparticles of a lower concentration in water (also stabilized by gelatin) was added for comparison. As obvious the absorption maximum was shifted to 415 nm which is not significant for the detection. None of the used electrolytes absorbed light in this range of wavelengths.

Transmission electron microscopy

Ag nanoparticles were studied using TEM micrographs (Fig. 4). The histogram of their sizes is shown in Figure 4c. Four main size fractions with the mean (median) values of 4 nm, 10 nm, 16 nm and 22 nm were recognized. The last and largest peak of the UV-VIS record in the system II (Fig. 1b) indicates that the predominating smallest nanoparticles had the lowest mobility. Based on this idea the average electrophoretic mobilities were correlated with the mean sizes of the Ag nanoparticles and the relationships with good linearity were obtained as shown in Figure 5. Most of papers describing separation of gold and silver nanoparticles reported the similar relationships.³¹⁻³³

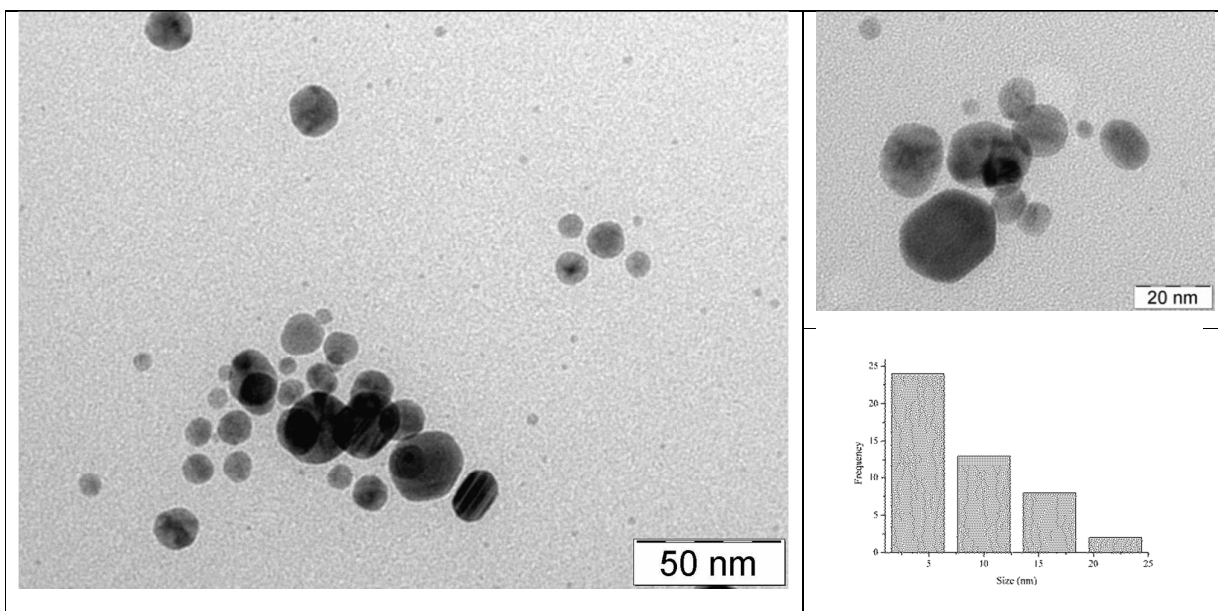


Figure 4 TEM micrographs of Ag nanoparticles. a) Micrograph with resolution of 50 nm, b) micrograph with resolution of 20 nm and c) histogram of Ag nanoparticles.

Electrophoretic mobility of Ag nanoparticles

As mentioned above, the ITP separation in the both electrolyte systems revealed the four zones mutually separated by other migrating zones acting as spacers. The number of separated Ag zones likely depends on the number of the spacers.

The better separation of all four Ag fractions was achieved in the system II with lower pHs of leading electrolyte and, thus, in all migrating zones. Ag nanoparticles were supposed to be covered by adsorbed gelatin polymers forming electric double layers. An isoelectric point of gelatin is about 4.5-5 and, therefore, the ionization at pH = 4.5 is lower than that at pH = 7.0. It follows from this adsorbed gelatin gave Ag nanoparticles different negative zeta potentials depending on a degree of ionization of gelatin function groups. This situation is similar to the separation of e.g. weak acids according to their pK.

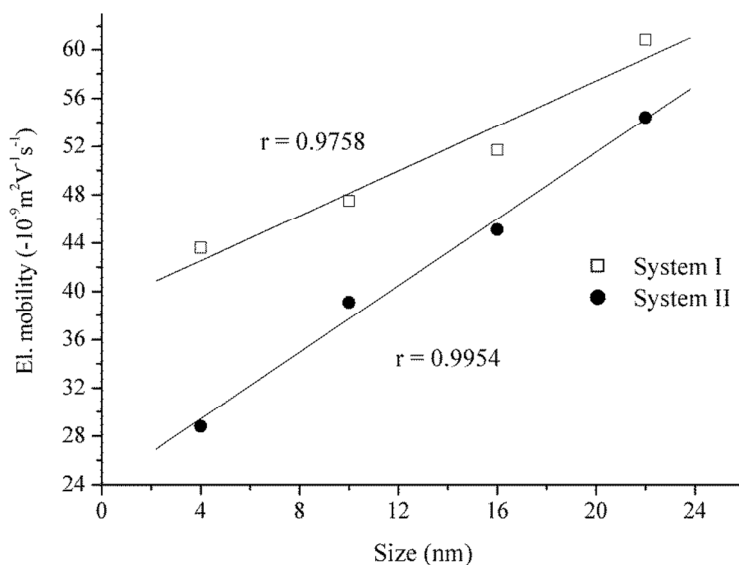


Figure 5 Dependence of average electrophoretic mobilities on mean Ag nanoparticles sizes (r – regression coefficient)

One of fundamental characteristics of the ITP separation of negatively charged species is elevating pH in their zones from leading to terminating one. In case of the separations shown in Figures 1a and 1b pH in the zones can be ordered as $\text{pH}(1) < \text{pH}(2) < \text{pH}(3) < \text{pH}(4)$. The data in Table II indicate that the electrophoretic mobilities decreased with increasing pH and, consequently, a degree of gelatin ionization. Therefore, the zeta potential of Ag nanoparticles expressed in Eq. (5) cannot play a decisive role for their ITP separation. In addition, the effect of pH on viscosity of gelatin solutions was experimentally verified but was found to be very low to influence the electrophoretic mobility of Ag nanoparticles.

In order to understand the ITP separation and to explain the role of gelatin, the hydrodynamic size and zeta potential measurements of the silver nanoparticles dispersions with different pH were performed (Tab. III). At $\text{pH} = 7.05$ gelatin formed larger structures with higher zeta potential than at $\text{pH} = 4.50$. The explanation is that at the higher pH the negative charges of gelatin chains caused stronger repulsion forces among them forming thicker gelatin double layers. This assumption was verified by the DLS experiments.

The gelatin double layer thickness $1/\kappa$ corresponding to $\text{pH} = 4.50$ and 7.05 can be simply estimated as the difference of the mean hydrodynamic radii determined by DLS of 61.5 nm and 144 nm and the mean nanoparticles radius estimated from the TEM images of *cca* 4 nm .

Table III Zeta potentials and mean hydrodynamic size of Ag/gelatin nanoparticles

pH	Zeta potential (mV)	Mean size (nm)
4.50	-7.3	123
7.05	-20.4	288

The $1/\kappa$ values were estimated at 57.5 nm and 140 nm, respectively. The corresponding $r\kappa$ values were calculated at 0.070 and 0.029 for pH = 4.5 and pH = 7.05, respectively. Therefore, we can conclude that the $r\kappa$ values corresponding to the ITP zones 1-4 can be order as $r\kappa(1) > r\kappa(2) > r\kappa(3) > r\kappa(4)$. Taking into account the electrophoretic mobilities in Tab. II this relation is in agreement with Eq. (5).

Both the zeta potential and the thickness of gelatin double layers, which determine mobility of Ag nanoparticles according Eq. (5), depends on ionization of gelatin function groups and thus on pH. Amount of adsorbed gelatin should depend on the size of nanoparticle and, therefore, we can suppose two basic variables influencing the ITP separation: i) size of Ag nanoparticles and ii) a degree of ionization of gelatin groups. In addition, mutual interactions of gelatin double layers of the nanoparticles can also influence their migration. As outlined above, the separation process is very complex to be unambiguously described. From the practical point of view, ITP was demonstrated to be an efficient tool for the separation of Ag nanoparticles according to their sizes.

Conclusion

Capillary isotachopheresis was used for the separation of silver nanoparticles stabilized by gelatin in ethanol-water colloid dispersions. The ITP separations were performed in the two separation systems with pH of the leading electrolytes of 7.1 (system I) and 4.5 (system II). In the isotachopheretic records the four peak-mode zones of Ag nanoparticles were identified at the boundaries of other ITP zones. The electrolyte system II provided the better separation.

The electrophoretic mobilities of the Ag nanoparticles varying from $-66.0 \times 10^{-9} \text{ m}^2\text{V}^{-1} \text{ s}^{-1}$ to $-25.7 \times 10^{-9} \text{ m}^2\text{V}^{-1} \text{ s}^{-1}$ were found to be proportional to the four size fractions of 4 nm, 10 nm, 16 nm and 22 nm evaluated from the TEM images. The DLS experiments demonstrated that thickness of gelatin double layers as well as zeta potentials depended on pH. Since the Ag nanoparticles migrated at the boundaries of other zones, these zones can be considered as the spacers necessary for the ITP separation.

The obtained experimental results showed that capillary isotachopheresis is able to separate the gelatine stabilized Ag nanoparticles according to their size due to different zeta potentials and thicknesses of the gelatin double layers. These findings extend common ITP applications from separation of organic and inorganic ions to separation of nanoparticles stabilized by polymers like gelatin. Based on these results off-line connections of ITP and/or ITP-CZE with TEM will be investigated in the future for the better characterization of metal and semiconductor nanoparticles.

Acknowledgement

This work was supported by the “National Feasibility Program I”, project LO1208 “TEWEP”, VŠB-Technical University of Ostrava (SP 2015/76) and by internal grant of Palacký University in Olomouc (IGA_PrF_2015_022). The authors thank Ales Panáček from the Department of Physical Chemistry, Faculty of Science, Palacký University in Olomouc for TEM measurements.

References

1. F. Kammer, S. Legros, E.H. Larsen, K. Loeschner and T. Hofmann, *Trends Anal. Chem.*, 2011, **30**, 425-436.
2. H. Kato, A. Nakamura, K. Takahashi and S. Kinugasa, *Nanomaterials*, 2012, **2**, 15-30.
3. H. Nolte, S. Schilde and A. Kwade, *Compos. Sci. Technol.*, 2012, **72**, 948-958.
4. K. Tiede, M. Hassellöv, E. Breitbarth, Q. Chaudhry and A. B.A. Boxall, *J. Chromatogr A*, 2009, **1216**, 503-509.
5. N. Surugau and P. L. Urban, *J. Sep. Sci.*, 2009, **2**, 1889-1906.
6. U. Pyell, W. Bücking, C. Huhn, B. Herrmann, A. Merkoulov, J. Mannhardt, H. Jungclas and T. Nann, *Anal. Bioanal. Chem.*, 2009, **395**, 1681-1691.
7. F. Sang, X. Huang and J. Ren, *Electrophoresis*, 2014, **35**, 793-803.
8. A. I. López-Lorente, B. M. Simonet and M. Valcárcel, *Trends Anal. Chem.*, 2011, **30**, 58-71.
9. M. Stanisavljevic, M. Vaculovicova, R. Kizek and V. Adam, *Electrophoresis*, 2014, **35**, 1929-1937.
10. Z. Zhang, F. Zhang and Y. Liu, *J. Chromatogr. Sci.*, 2013, **51**, 666-683.
11. I. Llorente, S. Fajado and J. M. Bastidas, *J. Solid State Electrochem.*, 2014, **18**, 293-307.

12. S. Oszwaldowski, K. Zawistowska-Gibuła and K. P. Roberts, *Anal. Bioanal. Chem.*, 2011, **399**, 2831-2842.
13. D.T.R. Stewart, M.D. Celiz, G. Vicente, L.A. Colón and D.S. Aga, *Trends Anal. Chem.*, 2011, **30**, 113-122.
14. F. Kitagawa and K. Otsuka, *J. Chromatogr. A*, 2014, **1335**, 43-60.
15. W. Bücking, O. Ehlert, J. Riegler, Ch. Rettenmeier, A. Merkoulov and T. Nann, *Int. J. Nanotechnol.*, 2007, **4**, 298-308.
16. W. Bücking and T. Nann, *IEE Proc. -Nanobiotechnol.*, 2006, **153**, 47-53.
17. W. Bücking, S. Massadeh, A. Merkulov, S. Xu and T. Nann, *Anal. Bioanal. Chem.*, 2010, **396**, 1087-1094.
18. A. Hlaváček and P. Skládal, *Electrophoresis*, 2012, **33**, 1427-1430.
19. U. Pyell, *Electrophoresis*, 2010, **31**, 814-831.
20. P. Praus, *Talanta*, 2005, **65**, 281-285.
21. G. Goet, T. Baier and S. Hardt, *Biomicrofluids*, 2011, **5**, 14109-14116.
22. J. Soukupová, L. Kvítek, A. Panáček, T. Nevěčná and R. Zbořil, *Mat. Chem. Phys.*, 2008, **111**, 77-81.
23. E. D. Ščukin, A. V. Percov and E. A. Amelinová, *Colloid Chemistry*, Academia, Prague, 1990.
24. R. J. Hunter, *Foundations of Colloid Science*, 2 nd Edition, Oxford University Press, New York, 2009.
25. P. H. Wiersema, A. L. Loeb and J. Th. Overbeek, *J. Colloid Interf. Sci.*, 1966, **22**, 78-99.
26. U. Schnabel, Ch. H. Fischer and E. Kendler, *J. Microcol. Sep.*, 1997, **9**, 529-534.
27. N. G. Vanifatova, B. Ya. Spvakov, J. Mattusch and R. Wennrich, *Talanta*, 2003, **59**, 345-353.
28. Y. Q. Li, H. Q. Wang, J. H. Wang, L. Y. Guan, B. F. Liu, Y. D. Zhao and H. Chen, *Anal. Chim. Acta*, 2009, **647**, 219-225.
29. M. Sivera, L. Kvítek, J. Soukupová, A. Panáček, R. Pucek, R. Večerová, R. Zbořil, *PLoS ONE*, 2014, **9**, e103675 (1-6.)
30. T. K. Khurana, J. G. Santiago, *Anal. Chem.*, 2008, **80**, 6300-6307.
31. F. K. Liu and G. T. Wei, *Anal. Chim. Acta*, 2004, **510**, 77-83.
32. F. K. Liu, Y. Y. Lin and C. H. Wu, *Anal. Chim. Acta*, 2005, **528**, 249-254.
33. F. K. Liu, M. H. Tsai, Y. C. Hsu, T. C. Chu, *J. Chromatogr. A*, 2006, **1133**, 340-346.